JOURNAL OF OPTOELECTRONICS AND ADVANCED MATERIALS Vol. 10, No. 5, May 2008, p. 1251 - 1256

Development of a technique for capturing Sleep Predictor Signals during wakefulness

E. FUJITA, Y. OGURA, N. OCHIAI, K. MURATA[a,*], T. KAMEI[a], Y. UENO[b], S. KANEKO[c]
Deltatooling Co., Ltd., 3-1 Taguchi-kenkyu-danchi, Higashi-hiroshima-shi, 739-0038 Hiroshima, Japan
[a]Shimane Institute of Health Science, 223-7 Enya-cho, Izumo-shi, 693-0021 Shimane, Japan; Kanazawa University Graduate School of Medical Science, 13-1 Takaramachi, Kanazawa-shi, 920-0934 Ishikawa, Japan
[b]Faculty of Engineering, Chiba Institute of Technology, 2-17-1 Tsudanuma, Narashino-shi, 275-0016 Chiba, Japan
[c]School of Engineering, The University of Tokyo, 7-3-1 Hongo, Bunkyo-Ku, 113-8656 Tokyo, Japan

The feature of sleep pattern is determined by the circadian rhythm that is typified by the rhythm of body temperature and homeostasis. In this study, a method was conceived for capturing changes in the peripheral circulatory system during the process of lowering of core body temperature via finger plethysmogram. Recorded signals were then analyzed by chaos analysis. By analyzing the variations in the time series of the gradients of the largest Lyapunov exponent and the power value (the square of the finger plethysmogram amplitude), and by observing the conditions of the subject, the phenomenon that predicts the subject's transition to Stage 1 sleep during wakefulness was detected. These predictive signals for falling asleep can be found when the amplitude of the power gradient was in transition, and when the largest Lyapunov exponent's gradient and the power gradient have an inverse phase with 180 degrees.

(Received March 13, 2008; accepted May 5, 2008)

Keywords: Sleep Prediction Signal, Sleep pattern, Circadian rhythm

1. Introduction

The mutual effects of an oscillator and homeostasis, which govern sleeping and waking rhythms, are made apparent in changes in the heartbeat, breathing, and body temperature. Fluctuation occurs within the variation in the heartbeat, breathing, and body temperature, and it was hypothesized that the progression from a waking state to a sleeping state could be observed by way of these fluctuations [1].

On one hand, the amplitude of the finger plethysmogram is governed by the heart's fluctuation characteristics; so is affected by contraction, expansion and variations in blood pressure. Furthermore, fluctuations in the baseline are due to fluctuation in the blood flow, which in turn translates into variations in the diameters of the skin's blood vessels. This is under the rule of the autonomic nerve system. This led us to hypothesize that indicators of a subject entering a sleep state are captured in the gradient time series wave form of the square of the amplitude of the finger plethysmogram pressure, and also are captured in the fluctuation in diameters of the blood vessels in the skin as evidenced in the largest Lyapunov value's gradient time series wave form and that indicators of entering a sleep state exist in the VLF and ULF [1,2], then the experiments on the sleep predictor during wakefulness by using finger plethysmogram, with the subjects in lying and sitting positions, were conducted.

2. Method

Sleep experiments were done in increments of 30 minutes, with the subjects lying down in a location that was quiet, had little vibration, was regulated for air circulation, temperature, and humidity, and had few power sources that would produce electrical hum. The experiments were done between 2:00 p.m. and 5:00 p.m., and the subjects were a male in his 40's and a female in her 30's (in order to verify any variances by gender), who both fall asleep within 10-15 minutes. The subjects' brain waves, eye movement, muscle electrograms, pulse, respiration, and finger plethysmograms were measured simultaneously.

In addition, gradient time series waveforms were measured by finger plethysmogram with the subjects in a sitting position, in a room with minimal vibration sources. These experiments were done on a male subject in his 40's and another male subject in his 60's, who both fell asleep within five minutes. The tests were conducted between the hours of 1:00 p.m. and 3:00 p.m.

3. Analysis methods

The give-and-take between the sleep-wakefulness rhythm and homeostasis can be seen in the state of blood flow to the skin, which is the one feedback mechanism of body temperature regulation. The dilation and contraction of blood vessels in the skin can be deduced by variations in the power value (the square of the amplitude of the finger plethysmogram waves) over a period of time. When evaluating by this variation, the start of data collection is the standard value, and the occurrence of variation is evaluated from that point on, and indices are created in

order that differences due to subject's health, the equipment being used, etc. may be absorbed.

Next, to explain the "largest Lyapunov exponent" of chaos dynamics, which is used in analyzing observations of emotional and physical states: the largest Lyapunov exponent is an index of orbital instability; the more stable the orbit, the smaller the number. When chaos analysis is done on a finger plethysmogram, the relation between the autonomous nervous system and the attractor's fluctuation [3,4] can be seen, as well as the relationship to the subject's emotional and physical states [5]. Based on these reports, it is understood that the largest Lyapunov exponent will be lower when the subject is relaxed, and that a higher number indicates the occurrence of adjustment, excitement, or concentration in the subject.

Symbols used

C_fk: Crest factor standard for waveform while awake
C_fs: Crest factor standard for Stage 1 sleep waveform
d: Parameter embedding dimension
$S(n)$: Finger plethysmogram time series signal
T_W: Timeframe for slide calculation: 180sec.
T_L: Overlap time (overlap of timeframe T_W and next timeframe T_W): 162sec
Xp: Time series waveform amplitudes indicating sleep predictors
Xk: Time series waveform amplitude, while subject is awake
Xs: Stage 1 sleep time series waveform amplitude
Δt: Time progression
λ: Largest Lyapunov exponent
τ: Embedding delay time

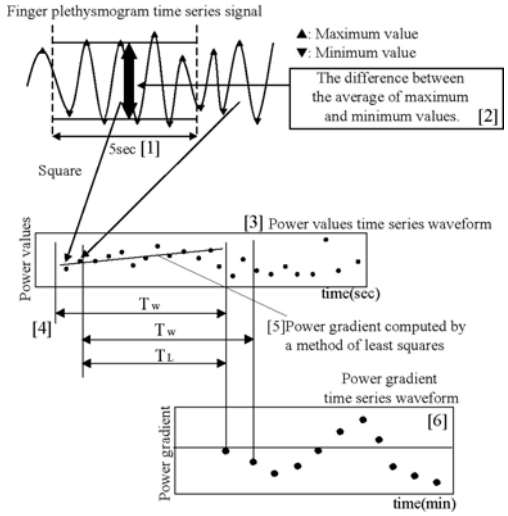

Fig. 1 The way to compute the time series of the power gradient.

Calculating the power gradient time series waveform

The method for calculating the power gradient time series waveform is shown in Fig. 1. The following steps (1) through (6) explain the calculation method for the corresponding values shown in Fig. 1. The Savitzky-Golay smoothing and differentiation method [6] is used to calculate the maximum and minimum values from the finger plethysmogram time series signals. Next, (1) the minimum and maximum values are divided at 5-second intervals, and each average value is computed. (2) The squares of the averages of each set of maximum and minimum values are the "power values". (3) The power values are plotted at 5-second intervals, creating the power value time series waveform.

In order to read large variations in the power value from this time series waveform, (4) the power value's gradient is computed across a given time frame T_W by the method of least squares (5).

The next timeframe T_W is then calculated in the same manner across overlap T_L and the results plotted. (6) These calculations (hereafter termed "slide calculations") are repeated to create the power gradient's time series waveform.

Computing the largest Lyapunov exponent gradient time series waveform

The following explains how the largest Lyapunov gradient time series waveform is computed, as it corresponds the values in Fig. 2, steps (7) through (15). (7) From time series signal $S(n)(n = 1,\ldots n)$, the time lag method[7] (Takens' embedding theory) is used to reconstruct the state of dynamic motion (parameter embedding dimension d, embedding time lag [7]). Specifically, only data $(S(i),S(i+\tau)),\ldots,S(i+(d-1))$ across the embedding dimension value within timeframe τ from the time series data start point is selected. (8) d factors are plotted as one point on the dimension d state space coordinate system. Plotting is accomplished by plotting i offset by one point each time. (9) The orbit described by this d dimension state space is the attractor. The finger plethysmogram timer series signal delay time is 50ms; when the FNN (False Near Neighbors) method [8] is used for the embedding dimension, FNN is near zero at dimension 3, and is exactly zero at dimension 4, so dimension 4 was seen as the optimum embedding dimension.

The largest Lyapunov exponent, which is one index that quantifies the quality of the attractor, is then calculated. The Lyapunov exponent is the averaged ratio of expansion and contraction of the attractor's orbit as it moves farther away, then draws closer again.

In this case, the Lyapunov exponent was computed using the Sano-Sawada method [9]. (10) As shown in Fig. 2, a "supersphere" is formed by certain points on the attractor; depending on time progression Δt, this supersphere may be elongated in one direction, or compressed in another direction, taking an elliptical shape. In other words, in this report the rate of change in direction of the 4 direct base vectors is defined as *e'i*, and when computed by random points on the attractor, the Lyapunov exponent is found using the formula below.

$$\lambda_i = \lim_{n\to\infty}\left(\frac{1}{n\Delta t}\right)\sum \log\left|e^{'}i(t)\right| \quad (1)$$

If the attractor's reconstructed state space is ***d*** dimension, then Lyapunov exponent ***λ1…λd*** is computed in relation to factor ***d***'s orthogonal vector. The one with the largest value within this area is the largest Lyapunov exponent. (11) The attractor is now reconstructed across an interval of 30 seconds based on calculations from the continuous data attained from the finger plethysmogram time series signals; by performing slide calculations at 1-second intervals, (12) the largest Lyapunov time series waveform is then created.

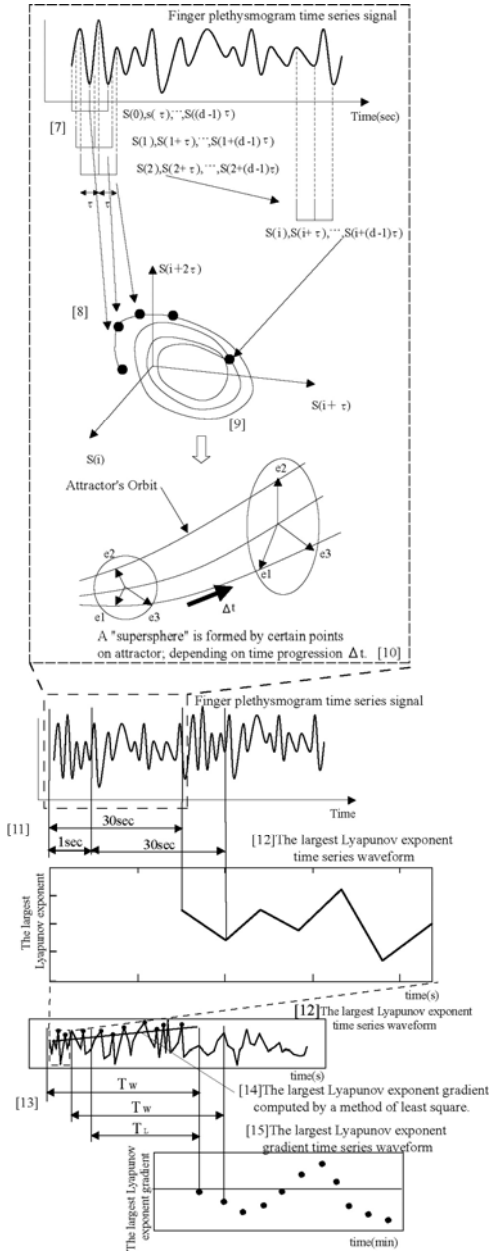

Fig. 2. The way to compute the time series of the largest Lyapunov exponent's gradient.

The maximum value in relation to the largest Lyapunov time series waveform can be found using the Savitzky-Golay smoothing and differentiation method [6]. In addition, variation of the largest Lyapunov exponent over an extended area can be found by finding the gradient of the largest Lyapunov exponent across timeframe T_W (13) by using the method of least squares on the computed maximum values (14). Next, the same calculations are done for the next timeframe T_W within the overlapping area T_L, and the results are plotted. (15) These calculations are repeated to create the largest Lyapunov exponent gradient time series waveform.

4. Results and discussion

The results of a male test subject in his 40's are shown in Fig. 3. In the first 14 minutes of the test, the brain waves showed a pattern of mixed waves, such as alpha waves and low-amplitude, high frequency beta waves, indicating the subject was awake. After 14 minutes, the amplitude of the alpha waves decreased, the frequency became somewhat slower, and the alpha waves gradually diminished, with waves in the 2-7 Hz range becoming prevalent; this indicated the 1st sleep stage had begun, in which the subject became sleepy and began nodding off.

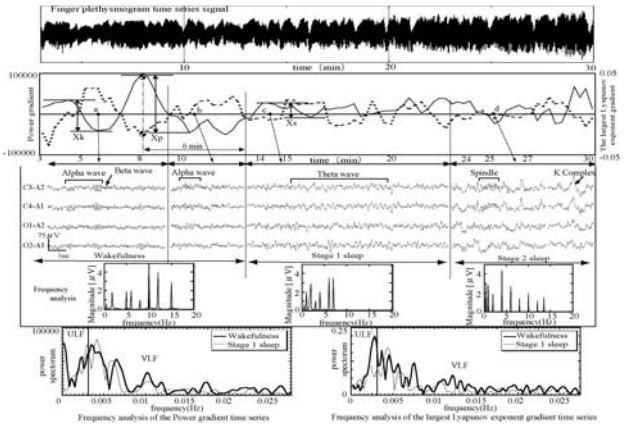

Fig. 3. Brain wave and the time series of the gradients of finger plethysmogram (male subject in his 40's).

After 24 minutes, sleep spindle and K compound waves began to appear, thought to be the 2nd sleep stage. The gradients of the power value and the largest Lyapunov exponent had an opposite phase state from a point 3 minutes into the experiment, and at around 8 minutes the amplitude reached its maximum height. This predicted the start of the 1st sleep stage that occurred 6 minutes later.

The area in which there is a large variance in the maximum and minimum values of the time series waveform, which depicts the power value and largest Lyapunov exponent gradients, and the area in which the cycles are long (0.0033-0.005Hz) and each gradient time series waveform is in an opposite phase state, are the areas defined as the transition state and called sleep predictor. In

this transition state, sympathetic nerve activity is weak and the skin's blood vessels begin to dilate; these phenomena are consistent with the increase in skin temperature before falling asleep. In addition, no clear gender differences were found in the occurrence of variations in the gradient time series waveforms computed from the finger plethysmogram data.

Then, a sleep experiment with the subjects in a sitting position was analyzed. Representative sleep predictors of the both subjects who fell asleep obediently (A zone) and resisted falling asleep (B zone) are shown in Figure 4. It was suggested that sleep predictor of the power spectrum of the subject who resisted falling asleep seemed to be larger than that of the subject who slept obediently. Moreover, it was regarded that the subject who resisted falling asleep had an increase in the amplitude of the largest Lyapunov exponent, and also the distribution rate of the beta wave [10]. In addition, these sleep predictors were close to 0.0033-0.005Hz (VLF, ULF) and seen only prior to the subject falling asleep for all the subjects.

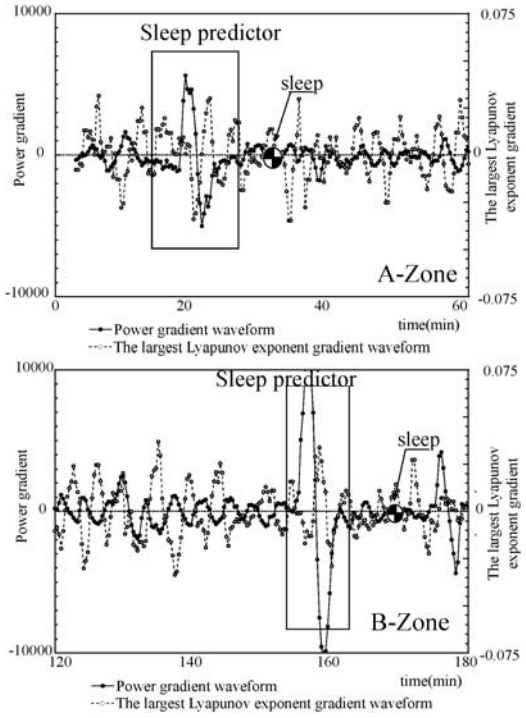

Fig. 4. Sleep predictors of falling asleep obediently (A zone) and resisted falling asleep (B zone).

5. Seat structures capturing biological signals

Fig. 5 shows the two seat structures that were developed to capture biological signals in a noninvasive manner: 3D net seat and full-formed seat. The two seat structures had the same sensor system: a magnetic circuit sensor for absorbing vibrations and detecting body movements, and an air pack sensor for detecting biological signals. Fig. 6 shows the vibration transmission characteristics of the seat shown in Fig. 5(b) due to vertical vibration input. When compared to the conventional full-formed urethane seat with the same structure, the present seat has improved vibration absorption near the resonance point. A decrease in the gain in the 5-8 Hz frequency zone causing visceral resonance is useful for capturing biological signals. Additionally, Fig. 7 shows the movements of the upper cushion frame due to the spring property of the torsion bar and the movements of the lower cushion frame due to floor vibration input in the form of frequency time-series waveforms. With a small vibration energy of up to 4 Hz, the upper and lower cushion frames moved in the same phase, but with a large vibration energy of ≥6 Hz, the upper and lower cushion frames moved in the opposite phases, thus lowering vibration energy. This demonstrates that the torsion bar structure is responsible for improving the vibration transmission characteristics, as shown in Fig. 6. Additionally, Fig. 8 shows the changes in the voltage and load of the magnetic circuit sensor. With the magnetic circuit sensor, the changes in load and voltage were linear, thus making it possible to detect the movements of a person in the seated position. Fig. 9 shows the original waveforms for body-trunk plethysmogram and respiration detected by the air pack sensor. Fig. 10 shows the results of frequency analysis. The above-mentioned results suggest that the present seat consisting of the air pack sensor and magnetic circuit sensor is capable of controlling vibrations and capturing biological signals.

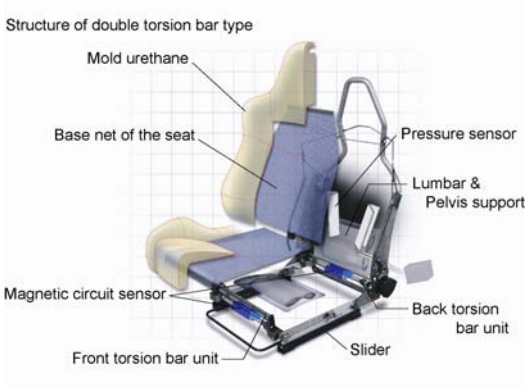

(a) Structure of the 3D Net seat

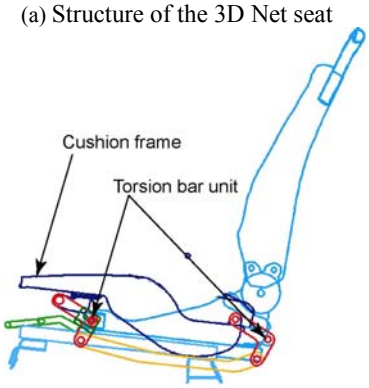

(b) Full-formed seat structure

Fig. 5. Seat structure.

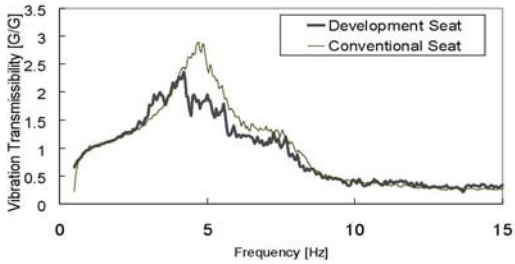

Fig. 6. Comparison of vibration transmission characteristics.

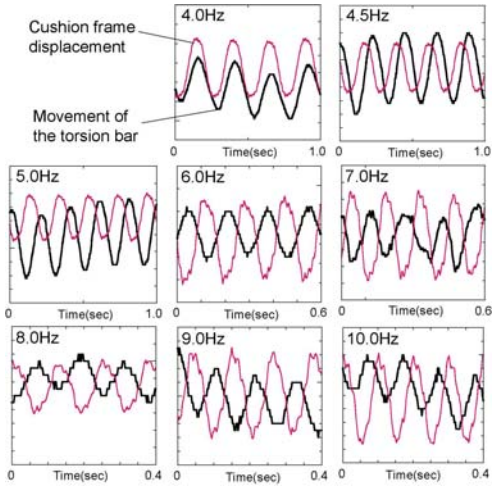

Fig. 7. Comparison of cushion displacement and torsion bar movement.

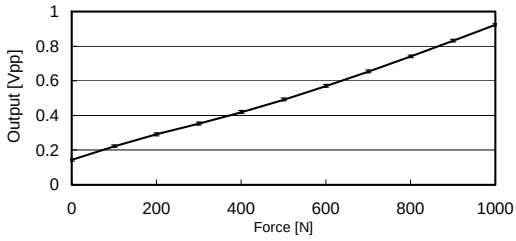

Fig. 8. Changes in the load and voltage of magnetic circuit sensor.

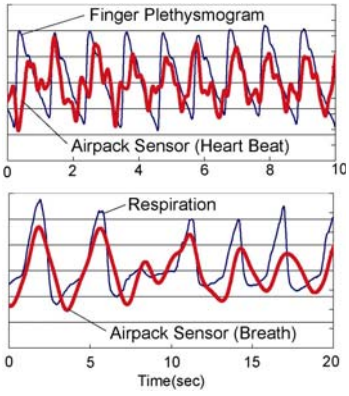

Fig. 9. Biological signals captured by the air pack sensor.

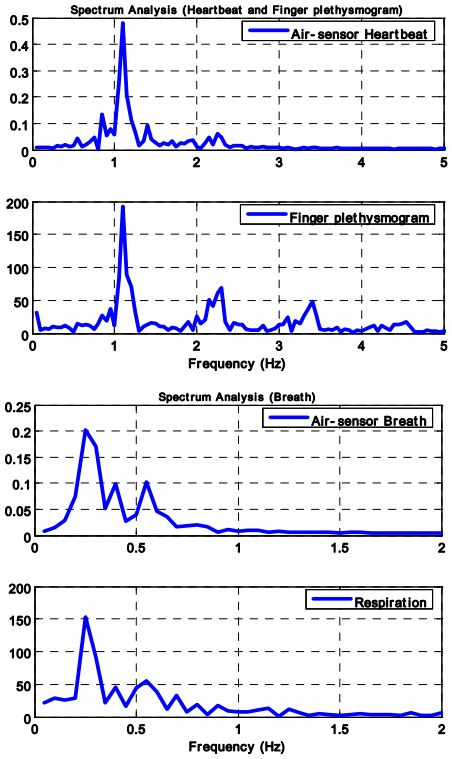

Fig. 10. Frequency analysis of biological signals captured using the air pack sensor.

6. Conclusions

Finger plethysmogram findings were compared to ECG findings, and it was possible to ascertain signs of falling asleep by plethysmography. In addition, we developed a seat made of an air pack sensor and a magnetic circuit sensor that can capture biological signals in the sitting position. In the future, we plan to verify whether or not these two sensor systems can noninvasively detect signs of falling asleep captured by a finger plethysmogram.

References

[1] E. Fujita, Y. Ogura, N. Ochiai, T. Miao, T. Shimizu, K. Murata, T. Kamei, Y. Ueno, S. Kaneko, Proceedings of VS TECH2005, JSME, No.05-202, 282-287 (2005).

[2] E. Fujita, Y. Ogura, N. Ochiai, T. Miao, T. Shimizu, T. Kamei, K. Murata, Y. Ueno, S. Kaneko, The Japanese Journal of Ergonomics, **41**(4), 203-212 (2005).

[3] T. Takemiya, T. Kinugasa, M. Miyasita, J. Maeda, H. Komiya, Japan Physiology Journal **47**(2), 65-76 (1995).

[4] M. Minami, A. Aimoto, M. Kabuto, Jpn. J. Hyg. **48**(2), 646-654 (1993).

[5] T. Miao, T. Shimizu, O. Shimoyama, Proceedings: Society of Automotive Engineers of Japan, No.18-3, 1-3, (2003).
[6] A. Savitzky, M. J. E.Golay, Analytical Chemistry, **36**, 1627-1639 (1964).
[7] K. Aihara, T. Ikeguchi, Y. Yamada, M. Komuro, Fundamentals and applications of chaos time series analysis, sangyo tosyo corp, 1-80, 2000.
[8] M. B. Kennel, R. Brow, H. D. I. Abarbanel, Phys. Rev. **A45**, 3403 (1992).
[9] M. Sano, Y. Sawada, Physical Review Letter **55**(10), 1082-1085 (1985).
[10] E. Fujita, Y. Ogura, N. Ochiai, E. Yasuda, S. Doi, K. Murata, T. Kamei, Y. Ueno, S. Kaneko, The Japanese Journal of Ergonomics **40**(5), 254-263 (2004).

*Corresponding author: murata6600@go9.enjoy.ne.jp